Thermomechanical analysis induced by interrupted cutting of Ti6Al4V under several cooling strategies

P. Lequien *, G. Poulachon (1), J.C. Outeiro (2)

Arts et Metiers, LaBoMaP Laboratory, UBFC, 71250 Cluny, France

ARTICLE INFO

Article history:
Available online 19 April 2018

Keywords:
Cryogenic machining
Thermal effects
Interrupted cutting

ABSTRACT

Cryogenic machining has mainly investigated in continuous cutting. Therefore, there is a lack of knowledge on the application of this technology to interrupted cutting, such as in milling. This study aims to investigate the thermomechanical phenomena in interrupted cutting of Ti6Al4V alloy under cryogenic, flood cooling and dry conditions. Due to the complexity of the thermomechanical analysis in milling, a special designed experimental setup has been developed through interrupted turning tests. This work highlights the influence of cryogenic flow rate and cutting time/non-cutting ratio on tool temperature. The obtained results can be extrapolated to milling operation.

1. Introduction

Machining refractory alloys generate high localized temperatures due to their poor thermal conductivity, high friction coefficient and high sensitivity to strain and strain-rate. As a consequence, rapid tool wear and poor surface integrity is observed when machining such alloys [1–3]. Several coolant strategies and/or machining assistances, including cryogenic assisted machining and tool vibration, can be applied to reduce these problems [4,5]. Indeed, cryogenic assisted machining, where liquid nitrogen (LN_2) is projected to the cutting zone, can be an effective solution to reduce the temperature in machining such alloys [6].

Challenges of cryogenic assisted machining are numerous and the cutting process of refractory alloys should be improved [7,8]. However, this poor controlled technology of liquid nitrogen deliverer to the cutting zone does not permit to compare all scientific works on cryogenic assisted machining, due to the scatter in the applied cooling conditions. In general, scientific publications agree on the benefit of LN_2 cooling in tool wear reduction, but show a scatter in terms of thermal phenomena and workpiece's surface integrity [9,10].

Several strategies to supply LN_2 to the cutting zone can be found in the literature. It seems that the most efficient way is to deliver LN_2 on the tool rake and flank faces, simultaneously [7]. Moreover, the efficiency of the cooling process depends on all LN_2 projection parameters, such as: flow rate, liquid/gas phase ratio, jet orientation and divergence, distance between the nozzle and the cutting zone. The convective heat transfer coefficient is a good indicator of this efficiency. Different convective heat transfer coefficients can be found in the literature without specifying all the LN_2 projection parameters [11,12]. The understanding of the physical phenomena during LN_2 projection is important to improve the efficiency of cryogenic assisted machining. LN_2 routing from the ranger to the nozzle has to be improved as well, in order to maximize the liquid/gas phase ratio at nozzle exit and to minimize the LN_2 loses [13].

Most of works on cryogenic assisted machining found in the literature are related with continuous cutting and very few of them deal with interrupted cutting [14]. In this case, many unknowns exist, including: the proper LN_2 routing system, the optimal LN_2 projection strategy and parameters, and their consequences in the cutting forces, tool wear and surface integrity.

The objective of the present work is to analyse the influence of LN_2 cooling on the tool temperatures and cutting forces in interrupted cutting of Ti6Al4V alloy, and compare it with dry and flood coolant conditions. In the case of milling, it's difficult to deliver the LN_2 through spindles and rotating tools, which requires particular precautions. Therefore, it seems to be easier to propose a thermomechanical analysis of interrupted cutting under cryogenic cooling conditions, using a fixed cutting tool and a workpiece shape. For such reason, interrupted turning tests are used to reproduce the milling operation.

2. Experimental set-up and parameters

Fig. 1 shows the experimental setup used in turning tests of Ti6Al4V alloy, using CNMG 120408 type uncoated cemented carbide cutting inserts. In order to deliver LN_2 at the cutting zone, a phase separator was used between the ranger and the tool holder. This phase separator is controlled using information from delivering temperature (at the phase separator exit) and LN_2 level

* Corresponding author.
E-mail address: pierre.lequien@ensam.eu (P. Lequien).

measurements. To ensure steady-state flow conditions, the LN_2 system (from the ranger to the nozzle) was cooled down before performing any test.

LN_2 is projected into both tool flank and rake faces using nozzles of different diameters. Variable nozzle diameters (1–3 mm) are used to spray LN_2 into the tool rake face, while a fixed nozzle diameter of 1.2 mm is used at tool flank face. The pressure was fixed at 2 bars. The average flow rate is determined by measuring the mass difference in the LN_2 ranger during the machining tests. These average flow rates are equal to 1.2, 1.9 and 2.5 l/min, corresponding to the nozzle diameters of 1, 2 and 3 mm, respectively.

Tool holder's internal channels for LN_2 delivering are previously optimized (by minimizing the angles through the flow), as well as the projection parameters (pressure, nozzle diameter, jet orientation and distance between the nozzle and the cutting zone), in order to maximize the convective heat transfer coefficient. In this case, LN_2 jet is oriented at $\alpha = 15^{\circ}$ and $\beta = 10^{\circ}$ in relation to the tool rake and flank faces, respectively (Fig. 1). The projection distance (d) is equal to 12 mm (Fig. 1).

A piezoelectric dynamometric (Kistler, model 9121) is used to measure the forces, while embedded thermocouples (TC_i) in the tool were used to measure the tool temperatures. Three thermocouples are placed in a hole having 0.5 mm of diameter and located at 1 mm beneath the tool rake face. The thermocouples (TC_1, TC_2 and TC_3 in Fig. 1) are placed in strategic positions in the tool, in order to compare the cooling influence on the tool temperature distribution.

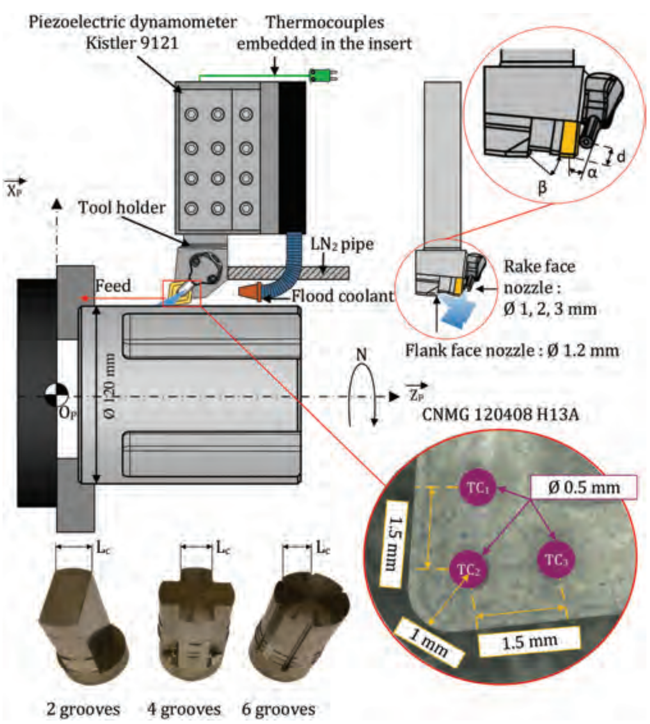

Fig. 1. Experimental set-up for interrupted turning tests of Ti6Al4V alloy.

Two kinds of experimental tests were carried out: (1) longitudinal turning tests over cylindrical workpieces, and (2) interrupted turning tests were performed on grooved workpieces (Fig. 1), to emulate a milling operation with a 40 mm milling cutter diameter (D). All of the samples have the same tool-workpiece engagement length (L_c) value of 31.4 mm, which is calculated by Eq. (1).

$$L_c = \frac{D}{2} \times arccos\left(1 - 2 \times \frac{a_e}{D}\right) \quad (1)$$

a_e is the radial depth of cut which is considered to be 0.5.D. Three workpieces of 120 mm diameter having 2, 4 or 6 grooves are designed, which are representative of the different frequencies of tool-workpiece engagement in milling operation (i.e. 5.3 H_z at $v_c = 30$ m/min and 9.7 Hz at $v_c = 55$ m/min with a 4 grooves workpiece). Cutting and non-cutting length ratio are 16%, 33% and 50% for 2, 4 and 6 grooves, respectively.

3. Results

3.1. Longitudinal turning tests

Priory to establish the design of experiments (DoE) for the interrupted turning tests, the determination of the restricted range of cutting conditions (v_c, f and a_p) for turning Ti6Al4V titanium alloy is mandatory. The minimum values of the cutting conditions can be determined by applying the methodology of minimal specific cutting forces (K_c) variation in function of the cutting conditions, according to the AFNOR standard NF E66-520-4-97. As an example, Fig. 2 shows the variation of K_c in function of f, keeping constant v_c and a_p. Applying the above-mentioned methodology, the minimum f to be used in the interrupted turning tests should be 0.125 mm.

Fig. 2 also provides information about the influence of the cooling strategy on K_c. Firstly, depending on the lubrication strategy, three sets of K_c curves can be identified, being flood coolant the current industrial reference for Ti6Al4V alloy machining. Secondly, for low LN_2 flow rates (1.2 l/min), which corresponds to near dry machining, the corresponding K_c curves (set 1) are below the flood one. However, K_c increases with the LN_2 flow rate (from 1.2 l/min, corresponding to set 1, to 1.9 l/min, corresponding to set 2). K_c will increase even more when LN_2 is projected on both tool rake and flank faces, simultaneously (set 3). Therefore, the projection of LN_2 on tool flank face has a non-negligible effect on K_c. In total, K_c increases 1.5 times from set 1 to set 3. This is due to the variation of the Ti6Al4V mechanical behavior and tribological conditions induced by the cooling strategies [7]. In particular, a possible increase of work material hardening while machining using high LN_2 flow rate.

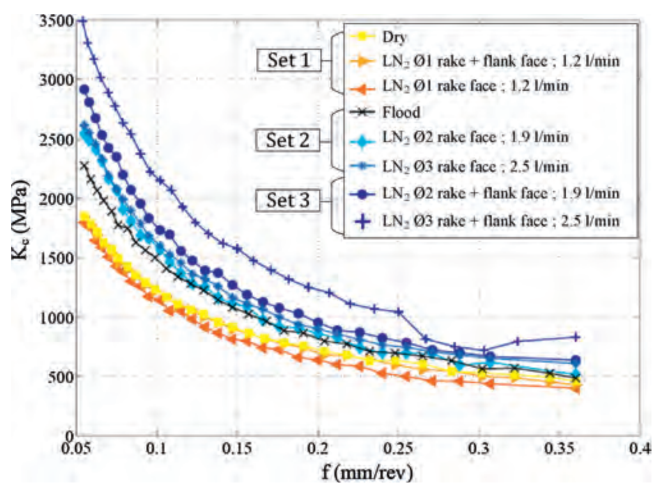

Fig. 2. Specific cutting forces (K_c) vs. feed (f) ($v_c = 55$ m/min, $a_p = 1$ mm).

3.2. Interrupted turning tests

Based on previous machining tests results, the following DoE for the interrupted turning is proposed. Four mains factors with two levels are chosen and presented in Table 1.

The LN_2 was projected simultaneously on both tool rake and flank faces. The measured parameters are the tool temperatures recorded by thermocouples (T_{TC1}, T_{TC2} and T_{TC3}) and the cutting (F_c), feed (F_f) and penetration (F_p) forces.

Fig. 3 shows the results for a workpiece with 4 grooves. This figure points out an increase of the maximal cutting forces (Fig. 3a)

Table 1
Factors and levels used in the DoE of interrupted turning tests.

Cooling conditions	Cutting conditions	
Dry	v_c (m/min)	30 and 55
Flood (6% oil at 2 bars)	f (mm)	0.1 and 0.2
LN_2 (rake and flank faces; nozzle Ø of 1 and 3 mm)	a_p (mm)	1
Number of workpiece grooves	2, 4 and 6	

and a decrease of the tool temperatures as the LN_2 flow rate increases (Fig. 3b). It appears that F_p and T_{TC2} are the most sensitive parameters to the cooling conditions. Therefore, further analysis will be focused only on the influence of LN_2 cooling on F_p and T_{TC2}.

Fig. 4 aims to show the variation of F_p and T_{TC2} signals during an interrupted turning test. Fig. 4b shows the decrease of T_{TC2} signal during machining. Temperature T_{TC2} stabilization appears after 40 s of machining.

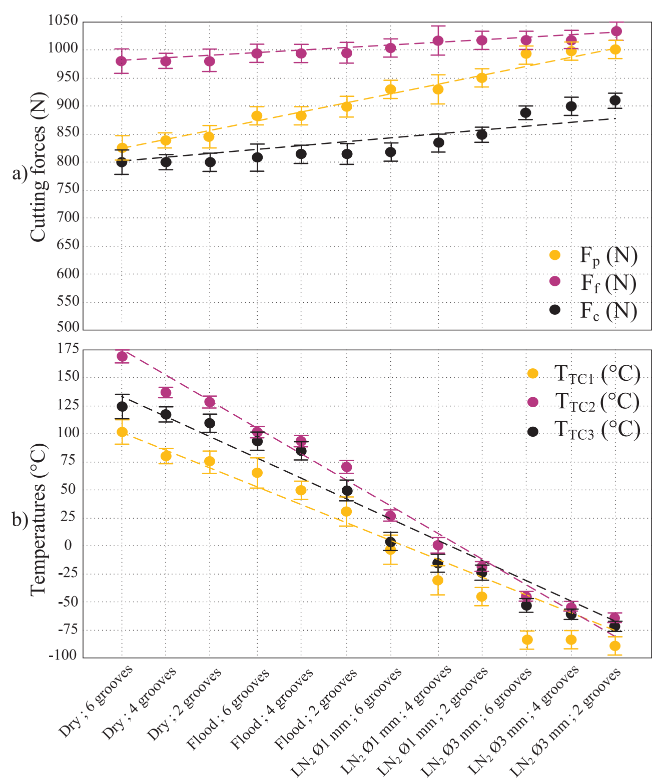

Fig. 3. Maximal forces (a) and temperatures (b) recorded during interrupted turning tests (v_c = 55 m/min, f = 0.2 mm/rev).

Fig. 4 zooms both F_p and T_{TC2} signals for one workpiece revolution. It is possible to point out a delay of 0.15 s between the sudden increase of F_p, when the tool become in contact with the workpiece, and the maximum generated T_{TC2}. The thermocouple response time is 0.05 s, which is negligible when compared to the observed delay between the force and temperature signals. So, this delay is probably due to the low thermal diffusivity of Ti6Al4V.

Fig. 5 represents the evolution of both F_p and T_{TC2} in function of the number of grooves. This figure shows that the number of grooves does not affect F_p, but it affects T_{TC2}. This temperature increases with the number of grooves. Increasing the number of grooves will increase the length of the tool cutting edge engaged in the workpiece and reduces the toolpath length between two consecutive workpiece tracks. Therefore, for the same cutting speed, increasing the number of grooves will increase the ratio between the cutting time and the non-cutting. Thus, more heat is generated by cutting and less time is available to cool down the tool before cutting the next track.

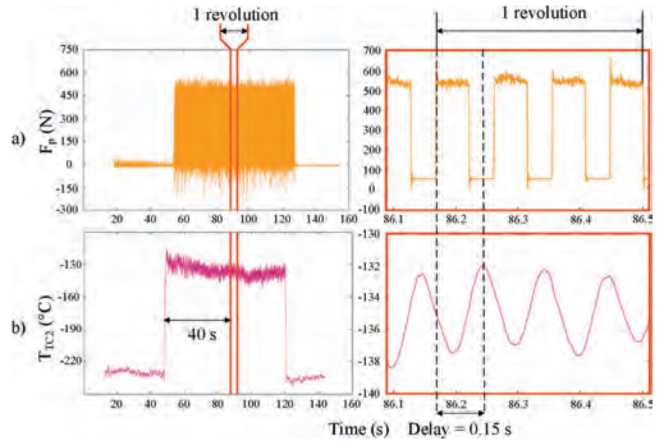

Fig. 4. Variation of F_p and T_{TC2} signals during an interrupted turning test (4?grooves workpiece, v_c = 55 m/min, f = 0.2 mm, LN_2 with Ø3 mm nozzle).

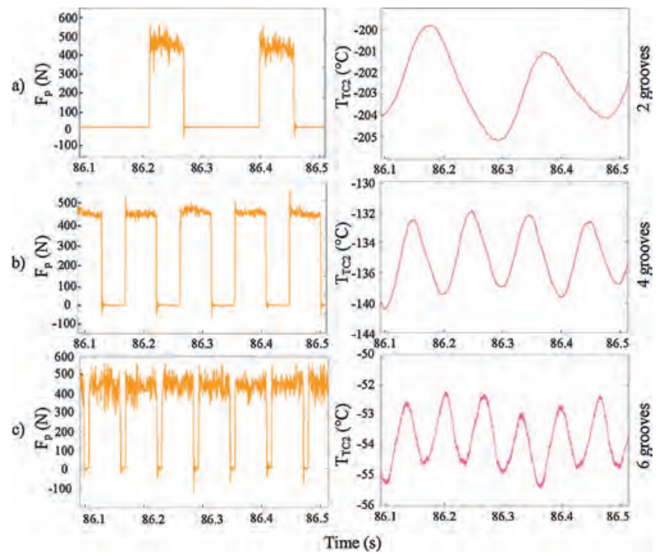

Fig. 5. Evolution of F_p and T_{TC2} as a function of workpiece grooves number (v_c = 55 m/min, f = 0.2 mm/rev, LN_2 with Ø3 mm nozzle).

Fig. 6 shows the T_{TC2} peak temperature in function of the number of grooves, for several cooling strategies (Fig. 6a) and cutting conditions (Fig. 6b). Fig. 6 put in evidence that this temperature always increases with the number of grooves,

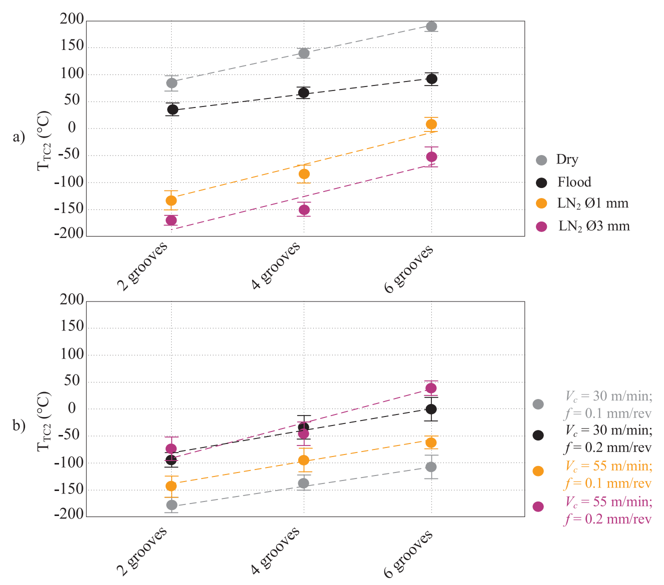

Fig. 6. T_{TC2} peak temperature in function of grooves number for several: (a) cooling strategies (v_c = 55 m/min, f = 0.2 mm); and (b) cutting conditions (LN_2 with Ø3 mm nozzle).

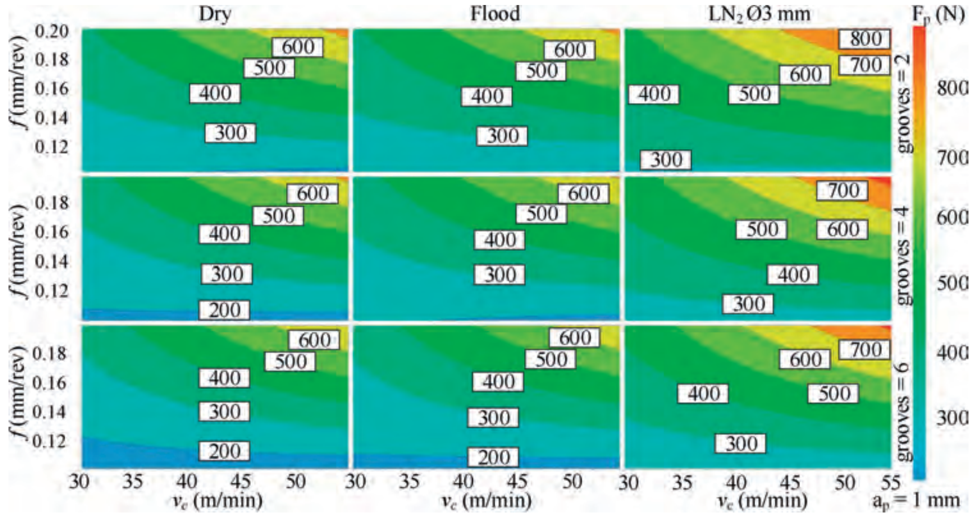

Fig. 7. 4D contour plot of F_p.

independently of the cooling strategy and cutting conditions. Moreover, lowest tool temperature is generated for LN_2 cooling at highest flow rate, and applying the lowest v_c and f values. This is due to smaller heat generated during cutting with the lowest v_c and f values, and the greater tool heat dissipation using the highest LN_2 flow rate.

In order to analyse all DoE results detailed in Table 1 and to present all the results in a single figure, a multilinear regression (MLR) analysis is applied as represented by the following general equation:

$$y_i = a_0 + a_1 x_{i,1} + a_2 x_{i,2} + \ldots + a_p x_{i,p} + \varepsilon_p; (i = 1, \ldots n) \quad (2)$$

where y_i is the total response, $x_{i,j}$ is the factor, a_0 the average value of the factor, $a_{i(i=1...4)}$ the polynomial coefficient, $a_{ij}.x_i.x_j$ are the interactions, and ε_p the residual. This equation can be expressed through a matrix of the DoE factors:

$$\begin{bmatrix} T_{TCi} \\ F_i \end{bmatrix} = \begin{bmatrix} x_{11} & \ldots & x_{1p} \\ x_{i1} & x_{ij} & x_{ip} \\ x_{n1} & \ldots & x_{np} \end{bmatrix} \begin{bmatrix} \text{No. grooves} \\ V_c \\ f \end{bmatrix} + \begin{bmatrix} \varepsilon_1 \\ \varepsilon_i \\ \varepsilon_n \end{bmatrix} \quad (3)$$

Applying the ANOVA analysis, it is possible to evaluate the influence of each factor in F_p, for each cooling strategy. A 4D contour plot is used to represent the results of this statistical analysis, as shown in Fig. 7. This figure shows that the highest F_p values are observed for LN_2 cooling, at high feeds and cutting speeds. This is possible due to an increase of work material hardening while machining using high LN_2 flow rate [7]. As already mentioned, the number of grooves does not affect F_p.

4. Conclusions

This paper presents thermomechanical analysis induced by dry, flood and LN_2 cooling conditions during machining of Ti6Al4V, using a special designed experimental set-up, combined with a statistical analysis of the results. Longitudinal turning tests showed that the specific cutting force is higher when LN_2 at high flow rate is projected on the tool rake and flank faces, simultaneously. The hypothesis of an increased work material hardening while machining using high LN_2 flow rate can be considered. In order to understand the influence of the cooling strategy in the thermomechanical phenomena in milling, simple interrupted turning tests were performed. These tests showed that the penetration force F_p is the most affected parameter by the cooling strategy, when compared to the other components of the resultant force. A statistical analysis showed that the highest F_p values are observed for LN2 cooling at high feeds and cutting speeds. Moreover, the number of workpiece grooves do not affect F_p, but it affects the tool temperature (T_{TC2}). This temperature always increases with the number of workpiece grooves, independently of the cooling strategy and cutting conditions. This is explained by an increase of the heat generated by cutting and less time to cool down the tool between tracks. These results can be extrapolated to milling operation.

Acknowledgments

The authors are very grateful to Professor Joël Rech for his participation in this research work. The authors also would like to thank the French Funds for Industrial and Innovation (F2I) for their financial support.

References

[1] Leyens C, Peters M, (Eds.) (2003), *Titanium and Titanium Alloys: Fundamentals and Applications*, Wiley-VCH, ISBN 3-527-30534-3.
[2] Rech J, Arrazola PJ, Claudin C, Courbon C, Pusavec F, Kopac J (2013) Characterisation of Friction and Heat Partition Coefficients at the Tool-work Material Interface in Cutting. *CIRP Annals—Manufacturing Technology* 62:79–82.
[3] M'Saoubi R, Outeiro JC, Chandrasekaran H, Dillon Jr OW, Jawahir IS (2008) A Review of Surface Integrity in Machining and Its Impact on Functional Performance and Life of Machined Products. *International Journal of Sustainable Manufacturing* 1:203–236.
[4] Bermingham MJ, Palanisamy S, Kent D, Dargusch MS (2012) A Comparison of Cryogenic and High Pressure Emulsion Cooling Technologies on Tool Life and Chip Morphology in Ti–6Al–4V Cutting. *Journal of Materials Processing Technology* 212:752–765.
[5] Paris H, Brissaud D, Gouskov A, Guibert N, Rech J (2008) Influence of the Ploughing Effect on the Dynamic Behaviour of the Self-vibratory Drilling Head. *CIRP Annals* 57:385–388.
[6] Hong SY, Markus I, Jeong W (2001) New Cooling Approach and Tool Life Improvement in Cryogenic Machining of Titanium Alloy Ti-6Al-4V. *International Journal of Machine Tools and Manufacture* 41:2245–2260.
[7] Jawahir IS, Attia H, Biermann D, Duflou J, Klocke F, Meyer D, Newman ST, Pusavec F, Putz M, Rech J, Schulze V, Umbrello D (2016) Cryogenic Manufacturing Processes. *CIRP Annals—Manufacturing Technology* 65:713–736.
[8] Yildiz Y, Nalbant M (2008) A Review of Cryogenic Cooling in Machining Processes. *International Journal of Machine Tools and Manufacture* 48:947–964.
[9] Courbon C, Kramar D, Krajnik P, Pusavec F, Rech J, Kopac J (2009) Investigation of Machining Performance in High-pressure Jet Assisted Turning of Inconel 718: An Experimental Study. *International Journal of Machine Tools and Manufacture* 49:1114–1125.
[10] Pusavec F, Krajnik P, Kopac J (2010) Transitioning to Sustainable Production—Part I: Application on Machining Technologies. *Journal of Cleaner Production* 18:174–184.
[11] Hriberšek M, Šajn V, Pušavec F, Rech J, Kopač J (2016) The Procedure of Solving the Inverse Problem for Determining Surface Heat Transfer Coefficient between Liquefied Nitrogen and Inconel 718 Workpiece in Cryogenic Machining. *Strojniški Vestnik—Journal of Mechanical Engineering* 62:331–339.
[12] Clausing AM (1990) Convective Heat Transfer Research Using a Cryogenic Environment. *Cryogenics* 30:335–340.
[13] Tahri C, Lequien P, Outeiro JC, Poulachon G (2017) CFD Simulation and Optimize of LN2 Flow Inside Channels Used for Cryogenic Machining: Application to Milling of Titanium Alloy Ti-6Al-4V. *Procedia CIRP* 58:584–589.
[14] Dhananchezian M, Pradeep Kumar M (2011) Cryogenic Turning of the Ti–6Al–4V Alloy with Modified Cutting Tool Inserts. *Cryogenics* 51:34–40.